

## SIGNIFICANT FINDINGS

for

### **Multi-Sensor Historical Climatology of Satellite-Derived Global Land Surface Moisture**

Manfred Owe, Richard de Jeu, and Thomas Holmes

A historical climatology of continuous satellite derived global land surface soil moisture is being developed. The data set consists of surface soil moisture retrievals from observations of both historical and currently active satellite microwave sensors, including Nimbus-7 SMMR, DMSP SSM/I, TRMM TMI, and AQUA AMSR-E. The data sets span the period from November 1978 through the end of 2006. The soil moisture retrievals are made with the Land Parameter Retrieval Model, a physically-based model which was developed jointly by researchers from the above institutions. These data are significant in that they are the longest continuous data record of observational surface soil moisture at a global scale. Furthermore, while previous reports have intimated that higher frequency sensors such as on SSM/I are unable to provide meaningful information on soil moisture, our results indicate that these sensors do provide highly useful soil moisture data over significant parts of the globe, and especially in critical areas located within the Earth's many arid and semi-arid regions.

## POPULAR SUMMARY

for

### **Multi-Sensor Historical Climatology of Satellite-Derived Global Land Surface Moisture**

Manfred Owe, Richard de Jeu, and Thomas Holmes

A historical database of land surface soil moisture derived from satellite data is being developed jointly by the NASA Goddard Space Flight Center and the Vrije Universiteit Amsterdam. This data set consists of surface soil moisture for all land areas of the Earth, and is derived from measurements taken by both historical satellites and currently active satellites. The data span the period from November 1978 through the present. The soil moisture values are derived with a model called the Land Parameter Retrieval Model, which was developed jointly by researchers from the above-mentioned institutions. It is expected that the data will be made available to the general science community within four to six months. Specifications and capabilities of the different satellite sensors and how they affect soil moisture retrievals are discussed in the paper. Examples of global patterns of surface soil moisture are also provided. These long-term data sets of global soil moisture may be helpful in many types of environmental monitoring studies.

# **Multi-Sensor Historical Climatology of Satellite-Derived Global Land Surface Moisture**

**Manfred Owe (1)**  
**Richard de Jeu (2)**  
**Thomas Holmes (2)**

- (1) Hydrological Sciences Branch  
NASA Goddard Space Flight Center  
Greenbelt, MD, USA
- (2) Dept. of GeoEnvironmental Sciences  
Vrije Universiteit Amsterdam  
Amsterdam, The Netherlands

## **Corresponding author address:**

Manfred Owe  
Mail Code 614.3  
NASA Goddard Space Flight Center  
Greenbelt, MD 20771, USA

Telephone: +1-301-614-5783  
FAX: +1-301-614-5808  
Email: [Manfred.Owe@nasa.gov](mailto:Manfred.Owe@nasa.gov)



1    **1. INTRODUCTION**

2

3    Land surface moisture is important in many Earth science disciplines. It is a key link between the  
4    land surface and the atmosphere. Soil moisture is an important parameter for many energy  
5    balance-related modeling applications, such as numerical weather forecasting, climate prediction,  
6    radiative transfer modeling, global change modeling, and other land processes models. Soil  
7    moisture usually exhibits a high degree of spatial variability. However, these spatial differences  
8    are not always entirely intuitive, and are a function not only of rainfall distributions, but are the  
9    result of topography, heterogeneity of soil physical properties, and land cover characteristics as  
10   well. Soil moisture has been identified as a parameter of considerable importance by the U.S.  
11   Global Change Research Program for improving the accuracy of large-scale land surface-  
12   atmosphere interaction models. Soil moisture is also thought to be the single most important  
13   parameter influencing the atmospheric circulation over land during the summer. Improved estimates  
14   of spatially representative surface moisture will significantly enhance both short and long-term  
15   precipitation forecasts. The soil surface is the transitional link between the soil water storage and  
16   atmospheric moisture. Surface soil moisture influences the partitioning of the incoming energy  
17   into latent and sensible heat components. Soil moisture, thus provides a key link between the  
18   water and energy balances.

19            From a historical perspective, researchers have had limited information about the large-  
20   scale distribution of soil moisture in time and space, since soil moisture is not routinely acquired  
21   like many hydrometeorological measurements. Consequently, long term observational data at the  
22   global scale, do not exist. While isolated observational data sets are available (Robock, 2000;  
23   Brock, 1995; Hollinger and Isard, 1994), they are largely regional in nature, and rarely extend

1 beyond several years duration. Furthermore, while in-situ observations are generally accurate,  
2 they still are point measures, and are not always readily transformed into spatial averages,  
3 especially at regional, continental, and global scales.

4 Space-based remote sensing offers potentially the greatest single contribution to large-  
5 scale monitoring of the Earth's surface. If properly utilized, satellite systems can offer the spatial,  
6 temporal, and spectral resolution necessary for consistent and continuous uninterrupted coverage  
7 of the whole Earth environment and its surrounding atmosphere. Such detailed observations are  
8 necessary in order to detect often-subtle environmental changes. Remote sensing technology is  
9 central to the integration of many interrelated but highly variable point scale phenomena to more  
10 useful, regionally-oriented land surface processes.

11 A historical data set of global surface soil moisture is being developed from satellite  
12 microwave brightness temperature observations. The data are derived from several different  
13 satellite sensors beginning in late 1978 and will continue to the end of 2006. The surface  
14 moisture retrievals are made with a Land Parameter Retrieval Model (LPRM), developed by  
15 researchers from the NASA Goddard Space Flight Center (GSFC) and the Vrije Universiteit  
16 Amsterdam (VU) (Owe et al., 2001). Because the data are derived from several sensors with  
17 different radiometric characteristics, some differences in sensing depth, spatial resolution, and  
18 orbit characteristics do exist. However, specifications for all sensors are well-documented in the  
19 literature, and a complete list of references is provided with the data. The data are expected to be  
20 available for download in 4 to 6 months, from the Goddard Earth Sciences Data and Information  
21 Services Center (GES DISC) and the Vrije Universiteit Amsterdam in The Netherlands. These  
22 data sets should prove valuable for many environmental modeling and monitoring applications.

## 2. GENERAL BACKGROUND

### 2.1 Soil Moisture Modeling and Retrieval

A variety of methods have been used to relate land surface wetness to passive microwave measurements. However, only a few modeling approaches can be considered true retrieval techniques. Results from early field and aircraft experiments demonstrated strong regression-based relationships between surface moisture and both brightness temperature and surface emissivity (Schmugge, 1976, 1978; Jackson et al., 1984). Models subsequently became more complex by accounting for canopy effects (Mo et al., 1982; Jackson et al., 1982; Jackson and Schmugge, 1991), roughness (Choudhury et al., 1979), polarization mixing (Wang and Choudhury, 1981), and other perturbing factors (Jackson and O'Neill, 1987; Jackson et al., 1992, 1997; O'Neill and Jackson, 1990). While many of these models are based on radiative transfer theory, an element of empiricism often remained because of difficulty in parameterizing some of these components from other biophysical measurements and at more meaningful spatial scales.

The lack of large scale surface moisture observations, has often forced researchers to calculate soil wetness indices from more readily-available meteorological data, for comparison to satellite observations (McFarland, 1976; Wilke and McFarland, 1986; Owe et al., 1988, Ahmed, 1995; Achutuni and Schofield, 1997). These approaches have successfully demonstrated the spatial and temporal sensitivity of satellite sensors, and have also been extremely useful for studying long term seasonal and interannual climatologies. However, wetness indices do not necessarily relate directly to actual surface moisture quantities, and therefore their value is limited for use in many environmental monitoring and modeling applications.

1            Satellite microwave observations have compared well with actual soil moisture  
2 measurements in several studies as well (Owe et al., 1992; Jackson, 1997; Drusch et al., 2001;  
3 Jackson and Hsu, 2001). However, an inherent problem with ground measurements has often  
4 been the issue of scaling point observations to sensor footprint-sized averages. This task becomes  
5 even more problematic in locations of heterogeneous land cover.

6            Several passive microwave modeling approaches have been developed that can be  
7 considered true retrieval techniques. McFarland and Neale (1991) developed a regression a  
8 technique that used brightness temperatures from several Special Sensor Microwave Imager  
9 (SSM/I) channels in a series of three empirical equations that accounted for different vegetation  
10 density classes. However, this approach calculated a soil wetness index, and was calibrated to  
11 regional Antecedent Precipitation Index calculations for test sites in the U.S. Southern Great  
12 Plains region. Errors associated with this method were also quite high. Its application to other  
13 locations and at global scales may therefore be less useful, especially in data-poor regions where  
14 validation attempts may be more difficult.

15            The retrieval model developed by Jackson (1993) has yielded extremely good results with  
16 aircraft data from several large field experiments (Jackson et al., 1995, 1999). The model has  
17 also performed well with Tropical Rainfall Measuring Mission (TRMM) Microwave Imager  
18 (TMI) and SSM/I measurements over these same experimental sites (Jackson and Hsu, 2001;  
19 Jackson et al., 2002). However, this approach requires a parameterization of the vegetation water  
20 content (VWC) in order to calculate the canopy optical depth (Jackson et al., 1982; Jackson and  
21 Schmugge, 1991). While extensive biophysical measurements were made throughout the test  
22 sites during these field experiments from which VWC could be calculated, it may be more  
23 difficult to obtain this information on a regular basis globally.



1           The method developed by Njoku (Njoku and Li, 1999; Njoku et al., 2003) is the official  
2 Advanced Microwave Scanning Radiometer (AMSR-E) soil moisture science team contribution  
3 (Njoku, 2004). This approach is based on polarization ratios, which effectively eliminate or  
4 minimize the effects of surface temperature. The original approach used six microwave channels  
5 (three frequencies, each at two polarizations) to solve for three land surface parameters (soil  
6 moisture, vegetation water content, and surface temperature). It was expected to provide surface  
7 soil moisture with an accuracy of 6 percent absolute moisture content ( $0.06 \text{ cm}^3 \text{ cm}^{-3}$ ) in areas  
8 with low vegetation biomass ( $< 1.5 \text{ kg m}^2$ ). However, unanticipated RFI problems were  
9 encountered at the 6.9 GHz frequency, requiring modification of the approach (see Njoku, 2004).

10           Another recently-developed retrieval approach is based on the microwave polarization  
11 difference index (Owe et al., 2001; De Jeu and Owe, 2003; Meesters, 2005). This method uses a  
12 forward modeling optimization procedure to solve a radiative transfer equation for both soil  
13 moisture and vegetation optical depth, and requires no calibration parameters or other  
14 biophysical measurements during the retrieval process. A unique feature of this approach is that  
15 it may be applied at any microwave frequency, and it was used in the retrieval of the data sets  
16 described in this paper. A more detailed description of this model is provided in Section 4.

17

## 18 **2.2 Sensors and Specifications**

19           The soil moisture data sets were derived from measurements obtained from a variety of  
20 satellite sensors beginning in late 1978. All sensors have several common wave bands, while  
21 some wave bands are either unique or common to only two or three of the satellite systems.  
22 Comparative specifications for the different sensors are provided in Tables 1 and 2. Brief

1 descriptions of the four sensors are provided, however, readers are referred to the various  
2 references provided for more a comprehensive discussion.

3 The Scanning Multichannel Microwave Radiometer (SMMR) was flown onboard the  
4 Nimbus-7 satellite (Gloersen and Barath, 1977; Gloersen et al., 1984). The instrument was  
5 launched in October 1978 and was eventually deactivated in August 1987. Power constraints  
6 onboard the Nimbus satellite permitted data acquisition on alternate days only, however, the 24  
7 hour on-off cycle still permitted both day and night observations. The satellite orbited the Earth  
8 approximately 14 times per day, with a local solar noon and midnight equator crossing. Because  
9 of the on-off instrument cycling, complete global coverage required 6 days. SMMR brightness  
10 temperatures were measured at five frequencies, from 6.6 GHz to 37 GHz, at both horizontal and  
11 vertical polarization. Spatial resolution of SMMR was comparatively coarse, relative to later  
12 instruments (from approximately 25 km at 37 GHz to almost 150 km at 6.6 GHz) (NSIDC,  
13 2005a).

14 The Special Sensor Microwave Imager (SSM/I) is found on board a series of Defense  
15 Meteorological Satellite Program (DMSP) platforms designated F-8, F-10, F-11, F-13, F-14, F-  
16 15, and F-16. The first satellite was launched in July 1987, while the last one was launched in  
17 October 2003. Orbit characteristics are very similar to Nimbus-7 (See Table 1). Equator crossing  
18 times vary between the different satellites and are provided in Table 3 (Armstrong et al., 1994;  
19 NSIDC, 2005b).

20 Tropical Rainfall Measuring Mission (TRMM) Microwave Imager (TMI) began  
21 acquiring data in December 1997. The TMI instrument is a nine channel radiometer, based  
22 largely on SSM/I technology. However, unlike the previous platforms, TRMM is in a near-  
23 equatorial orbit, so as to maximize observations over tropical ocean regions. Orbit characteristics

1 are less straight-forward than polar orbiting platforms. The satellite orbit is in a constant plane  
2 relative to the sun, with about 16 orbits per day. The Earth's inclination and rotation, therefore,  
3 results in a sine wave-like pattern of Earth coverage between about 38 degrees north and south  
4 latitude, with local overpass times drifting over the entire 24-hour day approximately once each  
5 month (TDIS, 2005; Kummerow, 1998).

6 The Advanced Microwave Scanning Radiometer (AMSR-E) on the AQUA Earth  
7 observation satellite was launched in May 2002. The sensor is 12 channels (six frequencies),  
8 with 4 bands relevant to soil moisture retrieval. Orbit characteristics are somewhat similar to its  
9 predecessor, SMMR, although the AMSR-E swath width is nearly twice as wide at 1445 km.  
10 Daily Earth coverage is nearly 100 percent above and below 45 degrees north and south latitude,  
11 while mid-latitudes experience about 80 percent coverage (Ashcroft and Wentz, 2003; NSIDC,  
12 2006).

13

### 14 **2.3 Data Archives**

15 All sensor data were downloaded as brightness temperatures from their public source  
16 archives. SMMR, SSM/I, and AMSR-E data are available from the National Snow and Ice Data  
17 Center (NSIDC) in Boulder Colorado (<http://nsidc.org/>). However, SSM/I brightness temperature  
18 data products are only available for the F-8, F-11, and F-13 satellites from NSIDC (2005b). TMI  
19 data were downloaded from the Goddard Earth Sciences Data and Information Services Center  
20 (GES DISC), formerly known as the Goddard Distributed Active Archive Center (DAAC)  
21 (<http://disc.sci.gsfc.nasa.gov/index.shtml>).

### 3. THEORETICAL BACKGROUND

Radiometric temperature readings have been shown to yield important information on moisture phenomena in the environment, including surface soil moisture. Microwave remote sensing is the only technology that provides a direct measure of the absolute moisture contained in the environment. Thermal radiation in the microwave region is emitted by all natural surfaces, and is a function of both the land surface and the atmosphere. The contribution of the atmosphere to the observed brightness temperature may be expressed as

$$T_{Bp} = T_u + \exp(-\tau_a)[T_{bp} + r_p T_d] \quad (1)$$

Where  $T_u$  and  $T_d$  are the upwelling and downwelling atmospheric emissions respectively,  $\tau_a$  is the atmospheric opacity,  $r_p$  is the surface reflectivity, and  $T_{bp}$  is the surface brightness temperature. The subscript  $p$  denotes either horizontal (H) or vertical (V) polarization. The surface brightness temperature is a function of the physical temperature of the radiating body and its emissivity, according to

$$T_{bp} \cong e_{sp} T_s \quad (2)$$

where  $T_s$  is the thermodynamic temperature of the emitting layer, and  $e_{sp}$  is the smooth-surface emissivity. The emissivity may be further defined as

$$e_{sp} = (1 - R_{sp}) \quad (3)$$

1 where  $R_s$  is the smooth-surface reflectivity. The absolute magnitude of soil emissivity is lower at  
2 H polarization than at V polarization, however, the sensitivity to changes in soil moisture is  
3 considerably higher. Conversely, at V polarization, the sensitivity to surface temperature is  
4 greater. This phenomenon forms the basis for surface temperature retrieval techniques by  
5 microwave radiometry (Owe and Van de Griend, 2001).

6 Soil moisture retrieval from microwave measurements is made possible due to the large  
7 contrast between the dielectric constants of dry soil ( $\sim 4$ ) and water ( $\sim 80$ ). This contrast results in  
8 a broad range in the dielectric properties of soil-water mixtures (4 – 40), and is the primary  
9 influence on the natural microwave emission from the soil (Schmugge, 1985). The dielectric  
10 constant is defined as a complex number, where the real part determines the propagation  
11 characteristics of the energy as it passes upward through the soil, and the imaginary part determines  
12 the energy losses. In a heterogeneous medium such as soil, the complex dielectric constant is a  
13 combination of the individual dielectric constants of its constituent parts, and includes air, water,  
14 rock, etc. Other factors which will influence the dielectric constant are temperature, salinity, soil  
15 texture, and wavelength. The dielectric constant is a difficult quantity to measure on a routine basis  
16 outside the laboratory, and values are generally derived from models (Dobson et al., 1985; Wang  
17 and Schmugge, 1980).

18 Microwave energy originates from within the soil, and the contribution of any one soil layer  
19 decreases with depth. For practical purposes, the surface layer provides most of the measurable  
20 energy contribution and is defined as the thermal sampling depth (Schmugge, 1983), although, it  
21 also commonly referred to as the skin depth or observation depth. The thickness of this layer is  
22 thought to be only several tenths of a wavelength thick. However, its actual thickness will vary  
23 according to moisture content, wavelength, polarization, and incidence angle. As the average

1 moisture content of this layer decreases, its thickness increases. It is the average dielectric properties  
2 of this layer that determines the observed emissivity.

3 Vegetation affects the microwave emission as observed from above the canopy in two  
4 ways. First, vegetation will absorb or scatter the radiation emanating from the soil. Secondly, the  
5 vegetation will also emit its own radiation. These two effects tend to counteract each other. The  
6 observable soil emission will decrease with increased vegetation, while emission from the  
7 vegetation will increase. Under a sufficiently dense canopy, the emitted soil radiation will  
8 become totally masked, and the observed emissivity will be due largely to the vegetation. The  
9 magnitude of the absorption depends upon the wavelength and the water content of the  
10 vegetation. The most frequently used wavelengths for soil moisture sensing are in the L- and C-  
11 bandwidths (~1.4 and ~6 GHz respectively), with L-band sensors having greater penetration of  
12 vegetation. While observations at all frequencies are subject to scattering and absorption and  
13 require some correction if the data are to be used for soil moisture retrieval, shorter wave bands  
14 are more susceptible to vegetation influences. A variety of models have been developed to  
15 account for the effects of vegetation on the observed microwave signal, and range from empirical  
16 linear models (Jackson et al., 1982; Ahmed, 1995; Owe et al., 1988), to more physically-based  
17 radiative transfer treatments (Mo et al., 1982; Njoku and Li, 1999; Wigneron et al., 1995;  
18 Wegmuller et al., 1995).

19 The radiation from the land surface as observed from above the canopy may be expressed  
20 in terms of the radiative brightness temperature,  $T_{bp}$ , and is given as a simple radiative transfer  
21 equation (Mo et al., 1982),

22

23 
$$T_{bp} = T_S e_{rp} \Gamma_p + (1 - \omega_p) T_C (1 - \Gamma_p) + (1 - e_{rp}) (1 - \omega_p) T_C (1 - \Gamma_p) \Gamma_p \quad (4)$$

1 where  $T_S$  and  $T_C$  are the thermodynamic temperatures of the soil and the canopy respectively,  $\omega$   
2 is the single scattering albedo, and  $\Gamma$  is the transmissivity. The first term of the above equation  
3 defines the radiation from the soil as attenuated by the overlying vegetation. The second term  
4 accounts for the upward radiation directly from the vegetation, while the third term defines the  
5 downward radiation from the vegetation, reflected upward by the soil and again attenuated by the  
6 canopy. The transmissivity is further defined in terms of the optical depth,  $\tau$ , and incidence angle,  
7  $u$ , such that

$$\Gamma = \exp(-\tau/\cos u) \quad (5)$$

11 The optical depth is strongly related to the canopy density, and for frequencies less than  
12 10 GHz, it can be expressed as a linear function of vegetation water content (Jackson et al.,  
13 1982). Maximum values for  $\tau$  were found to be about 1.3 at C-band for a soybean canopy with a  
14 vegetation water content of about  $1.5 \text{ kg m}^{-2}$  (Mo et al., 1982). However, the same canopy yields  
15 an optical depth of only 0.35 at L-band. An optical depth of 1.3 translates to a transmissivity of  
16 about 0.13, which indicates minimal penetration of the soil signal through the canopy at C-band.  
17 Furthermore, it was shown that at C-band, the above-canopy signal becomes totally saturated at  
18 an optical depth of about 1.5 ( $\omega = 0.06$ ) in the horizontal channel, although for practical  
19 purposes, the sensitivity is already quite low above 0.75 (Owe et al., 2001). At low soil moisture  
20 conditions, this threshold is seen to occur even sooner. In another study, African savannas were  
21 found to exhibit an annual course for the optical depth that varied from about 0.4 to 0.7 (Van de  
22 Griend and Owe, 1994).

1 The single scattering albedo describes the scattering of the soil emissivity by the  
2 vegetation, and is a function of plant geometry. The scattering albedo may be calculated  
3 theoretically (Wegmuller et al., 1995), however, experimental data for this parameter are  
4 limited, and values for selected crops were found to vary from 0.04 to about 0.13 (Mo et al.,  
5 1982; Owe et al., 2001). Few values are found for natural vegetation. A 3-year time series of the  
6 scattering albedo at both 6.6 GHz and 37 GHz was calculated for an African savanna region  
7 (Van de Griend and Owe, 1994). The scattering albedo exhibited considerable variability during  
8 the period, although no relationship with vegetation biomass or other seasonal indicators was  
9 observed.

10 While there is some experimental evidence indicating possible polarization dependence  
11 of both the optical depth and the scattering albedo, these differences have been observed mainly  
12 during field experiments and over vegetation elements that exhibit some uniform orientation  
13 such as vertical stalks in tall grasses, grains, and maize (Wigneron et al., 1995; Wegmuller et al.,  
14 1995; Kirdiashev et al., 1979). However, the canopy and stem structure for most crops and  
15 naturally occurring vegetation are randomly oriented. Furthermore, the affects of any systematic  
16 orientation exhibited by vegetation elements would most likely be minimized at satellite scales  
17 (Owe et al., 2001).

18

19

#### 4. LAND PARAMETER RETRIEVAL MODEL

20

21 Polarization ratios, such as the Microwave Polarization Difference Index (MPDI)

22

23

$$\text{MPDI} = (T_{b(V)} - T_{b(H)}) / (T_{b(V)} + T_{b(H)}), \quad (6)$$



1 are frequently used to normalize for temperature dependence, resulting in a parameter that is  
2 quantitatively and more highly related to the dielectric properties of the emitting surface(s). At  
3 lower frequencies (longer wavelengths), the MPDI will contain information on both the canopy and  
4 the soil emission, and consequently the soil dielectric properties as well. The theoretical relationship  
5 between the MPDI, vegetation optical depth, and the soil dielectric constant (Owe et al., 2001;  
6 Meesters et al., 2005), forms the basis for LPRM optimization. The latter reference describes an  
7 analytical solution to this relationship, which improves the accuracy and overall efficiency of the  
8 retrieval algorithm, while also allowing one to change the scattering albedo “on the fly”.

9 The retrieval methodology then uses a nonlinear iterative procedure in a forward  
10 modeling approach to partition the surface emission into its primary source components, i.e. the  
11 soil surface and the vegetation canopy, and optimizes on the canopy optical depth and the soil  
12 dielectric constant. Once convergence between the calculated and observed brightness  
13 temperatures is achieved, the model uses a global data base of soil physical properties (Rodell et  
14 al., 2004) together with a soil dielectric model (Wang and Schmugge, 1980) to solve for the  
15 surface soil moisture. No field observations of soil moisture, canopy biophysical properties, or  
16 other observations are used for calibration purposes, making the model largely physically-based  
17 with no regional dependence and applicable at any microwave frequency suitable for soil  
18 moisture monitoring (i.e L-, C-, X-, or Ku-band).

19 The LPRM does not establish or assume a soil moisture sampling depth during retrieval  
20 calculations, nor is there a depth implied by the retrieval, other than in the estimation of an  
21 average thermodynamic temperature for the emitting layer, which is assumed to be  
22 approximately 3 tenths of the wavelength. It will be left to the individual investigator to make  
23 any further assumptions as to the soil moisture sampling depth, based on the sensor used and any

1 additional climate information that one may have available. Land surface temperature is derived  
2 directly from 37 GHz vertical polarization brightness temperature observations, in a manner  
3 similar to the original model description (Owe et al., 2001; Owe et al., 2005; O'Neill et al.,  
4 2006), although additional large scale field observations and experimental data were used to  
5 refine the original relationship. The most reliable emitting layer temperature estimates will occur  
6 during the nighttime because of increased thermal equilibrium conditions of the near-surface air,  
7 canopy, and surface soil. Daytime emitting layer temperatures are often more difficult to  
8 estimate because of intense surface heating. This is often the case in arid and semi-arid locations,  
9 but less of a factor in more temperate regions. However, even though comparisons between  
10 daytime and nighttime retrievals have shown good consistency, it is expected that nighttime  
11 retrievals will most likely have smaller temperature-related errors than daytime retrievals.

12

13 **Evaluation.** Surface moisture retrievals have been evaluated against observational and  
14 simulation data sets for a variety of test sites (e.g. Global Soil Moisture Data Bank, ECMWF,  
15 Oklahoma Mesonet, LIS/LDAS), and were found to compare reasonably well (Owe et al., 2001;  
16 De Jeu and Owe, 2003; O'Neill et al., 2006). Wagner et al. (2007) compared surface soil  
17 moisture derived by 4 different retrieval models with a dense network of surface soil moisture  
18 observations from central Spain, and found the LPRM to give among the best results. A  
19 prototype dataset has also been produced for the SMMR period with the original retrieval  
20 algorithm in 2001, and has been studied extensively by researchers in the Goddard Global  
21 Modeling and Assimilation Office with quite positive results (Reichle et al., 2004).

## 5. RETRIEVAL DATA SETS

The LPRM will be used to derive global surface soil moisture for the period November 1978 through December 2006. These datasets will be produced from brightness temperature observations acquired from all available active and historical sensors, including Nimbus-SMMR (1978–1987), DMSP-SSM/I (1987–Present), TRMM-TMI (1997–Present), and AQUA-AMSR-E (2002–Present). In cases where multiple sensors were/are active during the same time period, we will process all available observational data. We will also process multiple frequencies where a given sensor has more than one suitable waveband for soil moisture retrieval. (i.e. SMMR, AMSR-E). All retrieval data sets will be written and stored in Hierarchical Data Format (HDF), which is the accepted standard for all EOS data products. This will ensure maximum compatibility with other EOS-era data sets, and will also ensure maximum compatibility with GES DISC data formatting protocols. Furthermore, HDF retains the Coordinated Universal Time (UTC) time-stamp and geo-reference information of the original orbit data.

Since the soil moisture data are derived from several different satellite sensors with varying spatial resolution and radiometric frequency, investigators should exercise care in the interpretation of these data and when using them in specific applications. Certain land cover characteristics will increase the possible error in the data retrievals, and may include excessive surface roughness which affects a significant percentage of the pixel, gross topography such as steep mountainous terrain, significant amount of pixel area occupied by water (as well as coastal pixels), and heavy vegetation. One must consider the radiometric characteristics of the individual sensor in estimating the impact of error sources on the data retrievals. Radiometric frequency is the primary factor influencing a sensor's ability to retrieve soil moisture and determines its effective global coverage. A lower

1 frequency (longer wavelength) sensor will provide greater coverage for soil moisture retrieval  
2 than a sensor of higher frequency, largely due to its ability to penetrate denser vegetation  
3 canopies. It may also be helpful to use other datasets in the interpretation of soil moisture retrievals,  
4 for instance terrain and topographic maps, vegetation maps, and land use maps, many of which may  
5 be available as digital remote sensing products as well

6         It has been determined that radio frequency interference (RFI) may have a significant  
7 impact on both H and V polarization brightness temperatures at C-band, and to a lesser extent at  
8 X-band. RFI is usually caused by communications and broadcast signals, and frequently results  
9 in abnormally high brightness temperatures. While the existence of RFI has been known for  
10 some time, rigorous studies of this phenomenon in Earth observation data (AMSR-E) have only  
11 recently been reported (Li et al., 2004; Njoku et al., 2005). Similar studies should be conducted  
12 with other sensors to determine the extent of this problem in historical data as well. The presence  
13 of RFI in radiometer data may be identified from original brightness temperature values (Li et  
14 al., 2004). Radio frequency contamination in 6–7 GHz range is seen to be highly prevalent in the  
15 U.S., Southwest Asia, and the Middle East, with occurrences in Europe seemingly associated  
16 only with selected urban locations. RFI in the 10 GHz is less prevalent globally, but appears to  
17 be concentrated in several European locations, such as Italy and the United Kingdom (See Njoku  
18 et al., 2005).

19         Although the LPRM process does not screen for RFI specifically, the presence of RFI in  
20 the radiometer data is often observed by unusual retrieval values. Moreover, in the event of  
21 extreme RFI, the LPRM has difficulty achieving convergence, and will not calculate a retrieval  
22 value. This is subsequently indicated by a “non-data” value.

1 Data screening for the presence of snow or frozen soils is limited to the elimination of  
2 those pixels where the surface temperature is observed to be at or below 273 K, as determined by  
3 the model's temperature algorithm. All non-data pixels (i.e. water, snow, ice, frozen soils, non-  
4 convergence, etc.) will be assigned unique values in order to retain their identity.

5  
6 **5.1 Scanning Multi-channel Microwave Radiometer.** SMMR surface moisture retrievals are  
7 performed at 6.6, 10.7, and 18 GHz. C-band is most susceptible to RFI contamination and has  
8 been found to be quite wide-spread in many global locations for the AMSR-E period (see above).  
9 However, its prevalence during the SMMR period has not been fully established, and the  
10 availability of the longer wavelength retrievals for unaffected areas would seem to be highly  
11 valuable. As indicated earlier, X-band RFI has been detected in Europe in recent years as well.  
12 Consequently, conducting surface moisture retrievals at both bands will maximize global  
13 availability of these data. Furthermore, the availability of 18 GHz retrievals will also allow  
14 investigators to evaluate the higher frequency data relative to the contemporaneous longer  
15 wavelength retrievals. Such comparisons will permit improved interpretation of similar higher  
16 frequency surface moisture retrievals from SSM/I measurements during periods when longer  
17 wavelength data are unavailable (for example, during the period after the deactivation of SMMR  
18 and the launch of TRMM). Global maps of daytime and nighttime SMMR retrievals are  
19 provided, illustrating the extent of daily (24-hour) orbital coverage (**Figure 1**). Global coverage  
20 is achieved in about six days because of the sensor's availability only on alternate days.

21 Average monthly surface soil moisture maps for the 6.6, 10.7, and 18 GHz bands are also  
22 provided for comparison (**Figure 2**). Both the soil sampling depth and the sensor's ability to  
23 penetrate vegetation decreases with frequency, and a subsequent decrease in global coverage of

1 soil moisture is clearly observed as the frequency increases. Since all three frequencies are  
2 contained on the same sensor platform, more meaningful direct comparisons between the three  
3 wavebands may be possible with these data.

4  
5 **5.2 Special Sensor Microwave Imager.** SSM/I retrievals are performed from the end of the  
6 SMMR period to the beginning of the AMSR-E period in 2002. Even though TMI data are  
7 available beginning in 1997, global coverage does not extend beyond  $\pm 35^\circ$  N and S. Therefore,  
8 SSM/I will remain useful by providing soil moisture retrievals at those latitudes not covered by  
9 TMI. Daily SSM/I retrievals illustrate orbital coverage that is similar to SMMR, although swath  
10 widths of SSM/I are somewhat wider (**Figure 3**). Average monthly soil moisture retrievals also  
11 appear similar in their distribution, magnitude, and extent of coverage as previous SMMR  
12 retrievals at a similar waveband (**Figure 4**).

13  
14 **5.3 TRMM Microwave Imager.** The application of TMI soil moisture retrievals may potentially  
15 be somewhat more complex due to the TRMM orbit characteristics. Since TMI is not a polar  
16 orbiter, the timing of daily coverage over any geographic location appears less systematic and  
17 almost random, although actually it is not. Daily coverage of polar orbiters occurs at the same  
18 local solar time at any given longitude, as the platform orbits the Earth. Furthermore, daytime  
19 and nighttime coverage for polar orbiters are typically archived separately, and are indicated as  
20 either ascending or descending orbits, respectively. However, TRMM is in a low-inclination  
21 orbit, extending from  $\pm 38^\circ$  north and south, which does not lend itself well to such systematic  
22 separation. A series of selected daily orbit tracks (orbit Nos. 0, 2, and 4) is illustrated, and shows  
23 the timing and coverage characteristics of TMI throughout part of a 24-hour day (**Figure 5**). The

1 resulting map of daily soil moisture retrievals is also illustrated (**Figure 6**). Patchiness in daily  
2 observations is frequently observed, and will result from soil moisture differences during  
3 subsequent overlapping and intersecting orbits as a result of precipitation events or extreme  
4 drying conditions.

5

6 **5.4 Advanced Microwave Scanning Radiometer.** AMSR-E orbital coverage is similar to the  
7 other polar orbiting satellites, as illustrated in the daytime and nighttime surface soil moisture  
8 retrievals (**Figure 7**). The wider swath width, however, results in almost 100 percent daily global  
9 coverage when the ascending and descending orbits are combined. One must keep in mind,  
10 however, that day and night coverage occurs at 12 hour intervals, and that the inherent timing  
11 information associated with the daytime and nighttime orbits would be lost during compositing.  
12 Average monthly global surface soil moisture retrievals for July 2003 are also illustrated for both  
13 6.9 GHz and 10.7 GHz frequencies (**Figure 8**). From these two examples, it is observed that  
14 consistency between the two frequencies appears to be quite good. The presence of RFI is also  
15 seen to be greater in the C-band data, and is especially observed in the western and eastern  
16 portions of the U.S. These observations are also consistent with results found by Li et al. (2004).

17

18

19

## 6.0 SUMMARY AND DISCUSSION

20

21

22

23

A historical global soil moisture climatology is being developed from microwave  
radiometer measurements from multiple satellite sensors dating back to 1978. The surface  
moisture retrievals are derived with the Land Parameter Retrieval Model, and will be hosted at

1 the Goddard Earth Sciences Data and Information Services Center, formerly known as the  
2 Goddard Distributed Active Archive Center (DAAC), and at the Vrije Universiteit Amsterdam in  
3 The Netherlands. Data storage will be in HDF, which will maximize compatibility with other  
4 EOS era data sets. It is expected that these data will be available for user download via FTP  
5 within four to six months. The sensors used in deriving surface soil moisture vary in frequency  
6 from C-band to X-band to Ka-band, and users should understand the significance of wavelength  
7 differences in the interpretation of these data.

8         Although a number of satellite-based soil moisture data products have been developed in  
9 recent years, most are limited in their spatial and temporal coverage or limited to only the  
10 AMSR-E period. The new data set is a global product, and is consistent in its retrieval approach  
11 for the entire period of data record. It must be remembered the data retrievals are made from  
12 different sensors with somewhat different radiometric characteristics. This results in differences  
13 in thermal sensing depth, spatial resolution, acquisition times, and possibly other characteristics  
14 as well. While these data should prove useful for many types of environmental monitoring  
15 studies, users should exercise care in their interpretation, and especially in forming conclusions  
16 derived from long-term observational studies.



- 1 **Acknowledgements:** Support for various phases of this research was provided by the Modeling,
- 2 Analysis, and Prediction Branch of NASA Headquarters and the Department of Geo-
- 3 Environmental Sciences, Vrije Universiteit Amsterdam.

## REFERENCES

- 1
- 2
- 3 Achutuni, R. and R.A. Schofield, 1997, "The Spatial and Temporal Variability of the DMSP  
4 SSM/I Global Soil Wetness Index". In: American Met. Soc., 13th Conf. on Hydrology,  
5 Long Beach, CA, pgs 188-189.
- 6 Ahmed, N.U., 1995, "Estimating soil moisture from 6.6 GHz dual polarization, and/or satellite  
7 derived vegetation index". *Int. J. Remote Sens.*, **16(4)**:687-708.
- 8 Armstrong, R.L., K.W. Knowles, M.J. Brodzik and M.A. Hardman, 1994. (updated current year).  
9 *DMSP SSM/I Pathfinder daily EASE-Grid brightness temperatures*, June to September  
10 2001. Boulder, CO: National Snow and Ice Data Center. Digital media and CD-ROM.
- 11 Ashcroft, P., and F. Wentz, 2003. (updated daily). *AMSR-E/Aqua L2A Global Swath Spatially-  
12 Resampled Brightness Temperatures (Tb) V001*, September to October 2003. Boulder, CO,  
13 USA: National Snow and Ice Data Center. Digital media.
- 14 Brock, F. V., K. C. Crawford, R. L. Elliott, G. W. Cuperus, S. J. Stadler, H. L. Johnson and M.  
15 D. Eilts. 1995. "The Oklahoma Mesonet: A Technical Overview." *Journal of Atmospheric  
16 and Oceanic Technology*, **12**:5-19.
- 17 B.J. Choudhury, T.J. Schmugge, A.T.C. Chang and R.W. Newton, 1979, "Effect of surface  
18 roughness on the microwave emission from soils, *J. Geophys. Res.* **84**:5699-5705.
- 19 De Jeu, R.A.M. and M. Owe, "Further validation of a new methodology for surface moisture and  
20 vegetation optical depth", *Int. J. Remote Sens.*, **24**:4559-4578, 2003.
- 21 Dobson, M.C., F.T. Ulaby, M.T. Hallikainen and M.A. El-Rayes, 1985, "Microwave dielectric  
22 behavior of wet soil - Part II: Dielectric mixing models, *IEEE Trans. Geosci. Remote Sensing*  
23 **23**:35-46.

- 1 Drusch, M., E.F. Wood, and T.J. Jackson, 2001, "Vegetative and atmospheric corrections for the  
2 soil moisture retrieval from passive microwave remote sensing data: Results from the  
3 Sothern Great Plains Hydrology Experiment 1997", *J. Hydromet.* **2**:181-192.
- 4 Gloersen, P. and F.T. Barath, 1977, A scanning multichannel microwave radiometer for Nimbus-  
5 G and SeaSat-A", *IEEE J. Oceanic Engineering* **2**:172-178.
- 6 Gloersen, P. and 14 Others, 1984: A summary of results from the first Nimbus-7 observations, *J*  
7 *Geophys Res.* **89**, 5335-5344.
- 8 Hollinger, S.E. and S.A. Isard, 1994, A soil moisture climatology of Illinois, *J. of Climate* **7**:822-  
9 833.
- 10 Jackson, T.J. 1997. Soil Moisture Estimation Using Special Sensor Microwave/Imager  
11 Satellited Data Over a Grassland Region. *Water Resources Research* **18(6)**:1475-1484.
- 12 Jackson, T.J., T.J. Schmugge, and J.R. Wang, 1982, "Passive microwave sensing of soil moisture  
13 under vegetation canopies". *Water Resources. Res.*, **18(4)**:1137-1142.
- 14 Jackson, T. J., Schmugge, T. J. and O'Neill, P. E. 1984. Passive microwave remote sensing of  
15 soil moisture from an aircraft platform. *Remote Sensing of Environment*, **14**:135-152.
- 16 Jackson, T.J. and P.E. O'Neill, 1987, "Salinity effects on the microwave emission of soils",  
17 *IEEE Trans. Geosci. Remote Sens.* **GE-25(2)**:214-220.
- 18 Jackson, T.J. and T.J. Schmugge, 1991, "Vegetation effects on the microwave emission from  
19 soils", *Rem. Sens. Environ.* **36**:203:212.
- 20 Jackson, T.J., K.G. Kostov, and S.S. Saatchi, 1992, Rock fraction effects on the interpretation of  
21 microwave emission from soil, *IEEE Trans. Geosci. Rem. Sens.*, **30(3)**:610-616.

- 1 Jackson, T. J., Le Vine, D. M., Swift, C. T., Schmugge, T. J., and Schiebe, F. R. 1995. Large  
2 area mapping of soil moisture using the ESTAR passive microwave radiometer in  
3 Washita'92. *Remote Sensing of Environment*, **53**: 27-37.
- 4 Jackson, T.J., P.E. O'Neill, and C.T. Swift, 1997, Passive microwave observation of diurnal  
5 surface soil moisture, *IEEE Trans. Geosci. Rem. Sens.*, **35(5)**:184-194.
- 6 Jackson, T.J., D.M. Le Vine, A.Y. Hsu, A. Oldak, P.J. Starks, C.T. Swift, J.D. Isham, and M.  
7 Haken, 1999, "Soil moisture mapping at regional scales using microwave radiometry: The  
8 Southern Great Plains Hydrology Experiment", *IEEE Trans. Geosci. Rem. Sens.*  
9 **37(5)**:2136-2151.
- 10 Jackson, T.J. and A.Y. Hsu, 2001, "Soil moisture and TRMM microwave imager relationships in  
11 the Southern Great Plains 1999 (SGP99) Experiment", *IEEE Trans. Geosci. Rem. Sens.*  
12 **39(8)**:1632-1642.
- 13 Jackson, T.J., A.Y. Hsu, and P.E. O'Neill, 2002, "Surface soil moisture retrieval and mapping  
14 using high frequency microwave satellite observations in the southern great plains", *J.*  
15 *Hydromet.* **3(6)**:688-699.
- 16 Kirdiashev, K.P., A.A. Chukhlantsev and A.M. Shutko, 1979, "Microwave radiation of the Earth's  
17 surface in the presence of vegetation cover", *Radio Eng. Electronics*, **24**:256-264.
- 18 Kummerow, C., W. Barnes, T. Kozu, J. Shiue, and J. Simpson, 1998, "The Tropical Rainfall  
19 Measuring Mission (TRMM) sensor package", *J. Atm. Oceanic Tech.*, **15**:809-817.
- 20 Li, L., E.G. Njoku, E. Im, P.S. Chang, and K. St. Germaine, 2004, "A preliminary survey of  
21 radio-frequency interference over the U.S. in Aqua AMSR-E data", *IEEE Trans. Geosci.*  
22 *Rem. Sens.*, **42(2)**:380-390.

- 1 McFarland, M.J., 1976, The correlation of Skylab L-band brightness temperatures with  
2 antecedent precipitation”, Conf. On Hydromet., Am. Met. Soc., Boston.
- 3 McFarland, M.J. and C.M.U. Neale, 1991. ”Land parameter algorithm validation and  
4 calibration”. In: *DMSP Special Sensor Microwave/Imager Calibration/Validation*. Ed. by  
5 J.P. Hollinger. Naval Research Laboratory, Final Report Vol. II.
- 6 Meesters, A.G.C.A., R.A.M. de Jeu, and M. Owe, 2005, “Analytical derivation of the vegetation  
7 optical depth from the microwave polarization difference index”, *IEEE Trans. Geoscience  
8 and Remote Sensing*, **2(2)**:121-123.
- 9 Mo, T., B.J. Choudhury, T.J. Schmugge, J.R. Wang, and T.J. Jackson, 1982, A Model for  
10 Microwave Emission from Vegetation-Covered Fields. *J. Geophys. Res.* **87(C13)**:11,229-  
11 11,237.
- 12 Njoku, E., 2004. updated daily. AMSR-E/Aqua Daily L3 Surface Soil Moisture, V001, *National  
13 Snow and Ice Data Center*, Boulder, CO, USA. Digital Media.
- 14 Njoku, E., P. Ashcroft, T.K. Chan, and L. Li (2005): Statistics and global survey of radio-  
15 frequency interference in AMSR-E land observations, *IEEE Trans. Geosci. Rem. Sens.*,  
16 **43(5)**:938–947.
- 17 Njoku, E. and L. Li, 1999, Retrieval of land surface parameters using passive microwave  
18 measurements at 6-18 GHz, *IEEE Trans. Geosci. Rem. Sens.* **37**:79–93.
- 19 Njoku, E., T. Jackson, V. Lakshmi, T. Chan, and S.V. Nghiem (2003): Soil moisture retrieval  
20 from AMSR-E, *IEEE Trans. Geosci. Rem. Sens.*, **41(2)**, 215–229.
- 21 NSIDC, 2005a. “Nimbus-7 SMMR Pathfinder Daily EASE-Grid Brightness Temperatures”,  
22 *National Snow and Ice Data Center*, Boulder CO. Digital Media.

- 1 NSIDC, 2005b. "DMSP SSM/I Pathfinder Daily EASE-Grid Brightness Temperatures". National  
2 Snow and Ice Data Center, Boulder CO. Digital Media.
- 3
- 4 NSIDC, 2006. "Data Products and Services", National Snow and Ice Data Center, Boulder, Co.
- 5 O'Neill, P.E. and T.J. Jackson, 1990, Observed effects of soil organic matter content on the  
6 microwave emissivity of soils, *Remote Sens. Environ.* **31**:175-182.
- 7 O'Neill, P.E., E.G. Njoku, J. Shi, E.F. Wood, M. Owe, and B. Gouweleeuw, 2006. "Hydros Soil  
8 Moisture Retrieval Algorithms: Status and Relevance to Future Missions", Proc. IGARSS  
9 2006.
- 10 Owe, M., A.T.C. Chang, and R.E. Golus, 1988, "Estimating Surface Soil Moisture from Satellite  
11 Microwave Measurements and a Satellite-Derived Vegetation Index", *Remote Sensing of  
12 Environment*, **24**:331-345.
- 13 Owe, M., A.A. Van de Griend, and A.T.C Chang. 1992. Surface Moisture and Satellite Microwave  
14 Observations in Semiarid Southern Africa. *Water Resour. Res.* **28(3)**:829-839.
- 15 Owe, M. and A.A. Van de Griend, 2001, "On the Relationship Between Thermodynamic Surface  
16 Temperature and High Frequency (37 GHz) Vertical Polarization Brightness Temperature  
17 Under Semi-Arid Conditions". *Int. J. Remote Sensing*, **22(17)**:3521-3532.
- 18 Owe, M., R.A.M. de Jeu, and J. Walker, 2001, "A methodology for surface soil moisture and  
19 vegetation optical depth retrieval using the microwave polarization difference index", *IEEE  
20 Trans. Geosci. and Remote Sensing*, **39**:1643-1694.
- 21 Owe, M., T. Holmes, R. De Jeu, 2005, "A physically based model with remote sensing inputs for  
22 improved soil temperature retrievals", *Proceedings: International Symposium on Remote  
23 Sensing*, Vol. 5976, Int. Soc. for Optical Eng., Bellingham, WA.

- 1 Reichle, R., R.D. Koster, J. Dong, A. Berg, 2004. "Global Soil Moisture from Satellite  
2 Observations, Land Surface Models, and Ground Data: Implications for Data  
3 Assimilation." *J. Hydromet.* **5**:430-442.
- 4 Robock, Alan, Konstantin Y. Vinnikov, Govindarajalu Srinivasan, Jared K. Entin, Steven E.  
5 Hollinger, Nina A. Speranskaya, Suxia Liu, and A. Namkhai, 2000, "The Global Soil  
6 Moisture Data Bank", *Bull. Amer. Meteorol. Soc.*, **81**:1281-1299.
- 7 Rodell, M., P.R. Houser, U. Jambor, J. Gottschalck, K. Mitchell, C.J. Meng, K. Arsenault, B.  
8 Cosgrove, J. Radakovich, M. Bosilovich, J.K. Entin, J.P. Walker, D. Lohmann, and D.  
9 Toll, 2004, "The Global Land Data Assimilation System", *Bull. Amer. Meteor. Soc.*  
10 **85(3)**:381-394.
- 11 Schmugge, T.J., 1976, "Remote sensing of soil moisture", NASA/Goddard Space Flight Center,  
12 Document X-913-76-118, Greenbelt, MD, 21 pp.
- 13 Schmugge, T.J., 1977, "Remote sensing of surface soil moisture", *J. Appl. Met.* **17(10)**:1549-  
14 1557.
- 15 Schmugge, T.J., 1983, "Remote sensing of soil moisture: Recent advances", *IEEE Trans. Geosci.*  
16 *Remote Sensing* **21**:336-344.
- 17 Schmugge, T.J., 1985, Remote Sensing of Soil Moisture. In: Hydrological Forecasting. M.G.  
18 Anderson and T.P. Burt, eds. John Wiley, New York.
- 19 TSDIS, 2005. "TRMM Science Data and Information System", url:<http://tsdis.gsfc.nasa.gov/>,  
20 NASA Goddard Space Flight Center, MD. Digital Media.
- 21 Van de Griend, A.A. and M. Owe, 1994, "Microwave vegetation optical depth and inverse  
22 modelling of soil emissivity using Nimbus/SMMR satellite observations", *Meteorology and*  
23 *Atmospheric Physics*, **54**:225-239.

- 1 Wagner, W., V. Naeimi, K. Scipal, R. de Jeu, and J. Martinez-Fernandez, 2007. "Soil Moisture  
2 from Operational Meteorological Satellites", *Hydrogeology Journal*, (In Press).
- 3 J.R. Wang and B.J. Choudhury, 1981, "Remote sensing of soil moisture content over bare field at  
4 1.4 GHz frequency", *J. Geophys. Res.* **86**:5277-5282.
- 5 Wang, J.R., and T.J. Schmugge, 1980, "An empirical model for the complex dielectric permittivity  
6 of soil as a function of water content", *IEEE Trans. Geosci. Remote Sensing*, **18**:288-295.
- 7 Wegmuller, C. Maetzler, and E.G. Njoku, 1995, "Canopy opacity models". In: *Passive Microwave*  
8 *Remote Sensing of Land-Atmosphere Interactions*, B.J. Choudhury, Y.H. Kerr, E.G. Njoku,  
9 and P. Pamploni Eds. Utrecht, NL: VSP:375-387.
- 10 Wigneron, j.p., A. Chanzy, J.C. Calvet, and N Bruguier, 1995, "A simple algorithm to retrieve soil  
11 moisture and vegetation biomass using passive microwave measurements over crop fields".  
12 *Rem. Sens. Environ.*, **51**:331-341.
- 13 Wilke, G.D. and M.J. McFarland, 1986, "Correlations between Nimbus 7 Scanning Multichannel  
14 Microwave Radiometer (SMMR) data and an antecedent precipitation index", *J. Climate*  
15 *Appl. Met.*, **25**:227-238.

16



## FIGURE CAPTIONS

**Figure 1.** Twenty-four-hour day and night SMMR surface soil moisture retrievals for 7 July 1980.

**Figure 2.** Average monthly SMMR surface soil moisture retrievals at 6.6 GHz (top), 10.7 GHz (middle), and 18 GHz (bottom) for 7 July 1980.

**Figure 3.** Twenty-four-hour day and night global SSM/I surface soil moisture retrievals for 7 July 2003.

**Figure 4.** Monthly average global surface soil moisture for July 2003 as retrieved from SSM/I.

**Figure 5.** Selected TRMM orbit tracks during a 24-hour period, illustrating a typical pattern of daily coverage. A given daily pattern will repeat approximately every 47 days.

**Figure 6.** Twenty-four-hour and average monthly global surface soil moisture retrievals for 7 July (top) and July (bottom) 2003, derived from TMI at 10.7 GHz.

**Figure 7.** Twenty-four-hour global daytime and nighttime surface soil moisture retrievals at 6.9 GHz from AMSR-E.

**Figure 8.** Average monthly global surface soil moisture retrievals at 6.9 GHz (top) and 10.7 GHz (bottom) from AMSR-E for July 2003.

TABLES

Table 1. Specifications for the various microwave sensors used in deriving the soil moisture data sets.

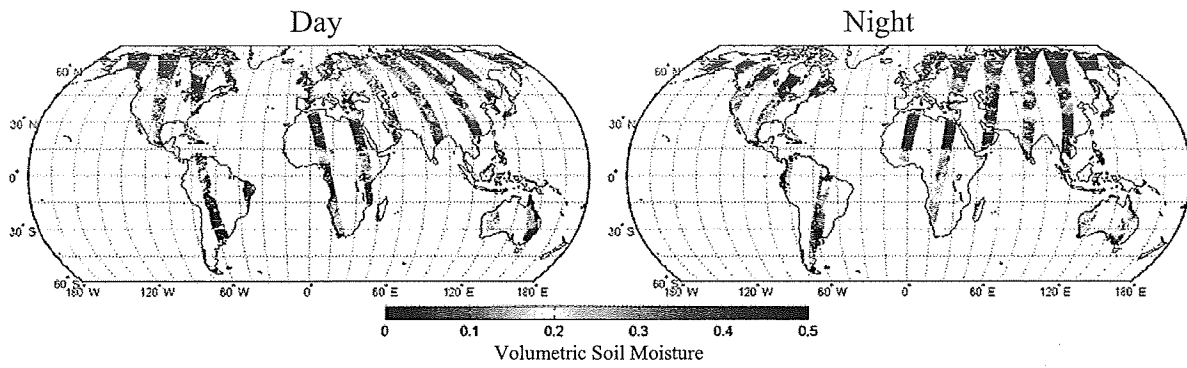
Parameter	SMMR	SSM/I	TMI	AMSR-E
Frequencies (GHz)	6.6, 10.7, 18, 37	19.3, 36.5	10.7, 19.4, 37	6.9, 10.7, 18.7, 36.5
Polarization	H,V all freq.	H,V all freq.	H,V all freq.	H,V all freq.
Incidence Angle	50.2°	53.1°	52.88°	55°
Swath Width (km)	780	1394	759	1445
Orbit Type	Polar	Polar	N35° to S35°	Polar
Equator Crossing				
Ascending Orbit	1200 LST	See Table 3	Variable	1330
Descending Orbit	2400 LST	See Table 3	Variable	0130
Data Period	Nov 1978 – Aug 1987	Jul 1987 - Present	Dec 1997 – Present	May 2002 – Present

Table 2. Footprint dimensions corresponding to the different sensors at all wavelengths relevant to soil moisture retrieval (along track x cross track).

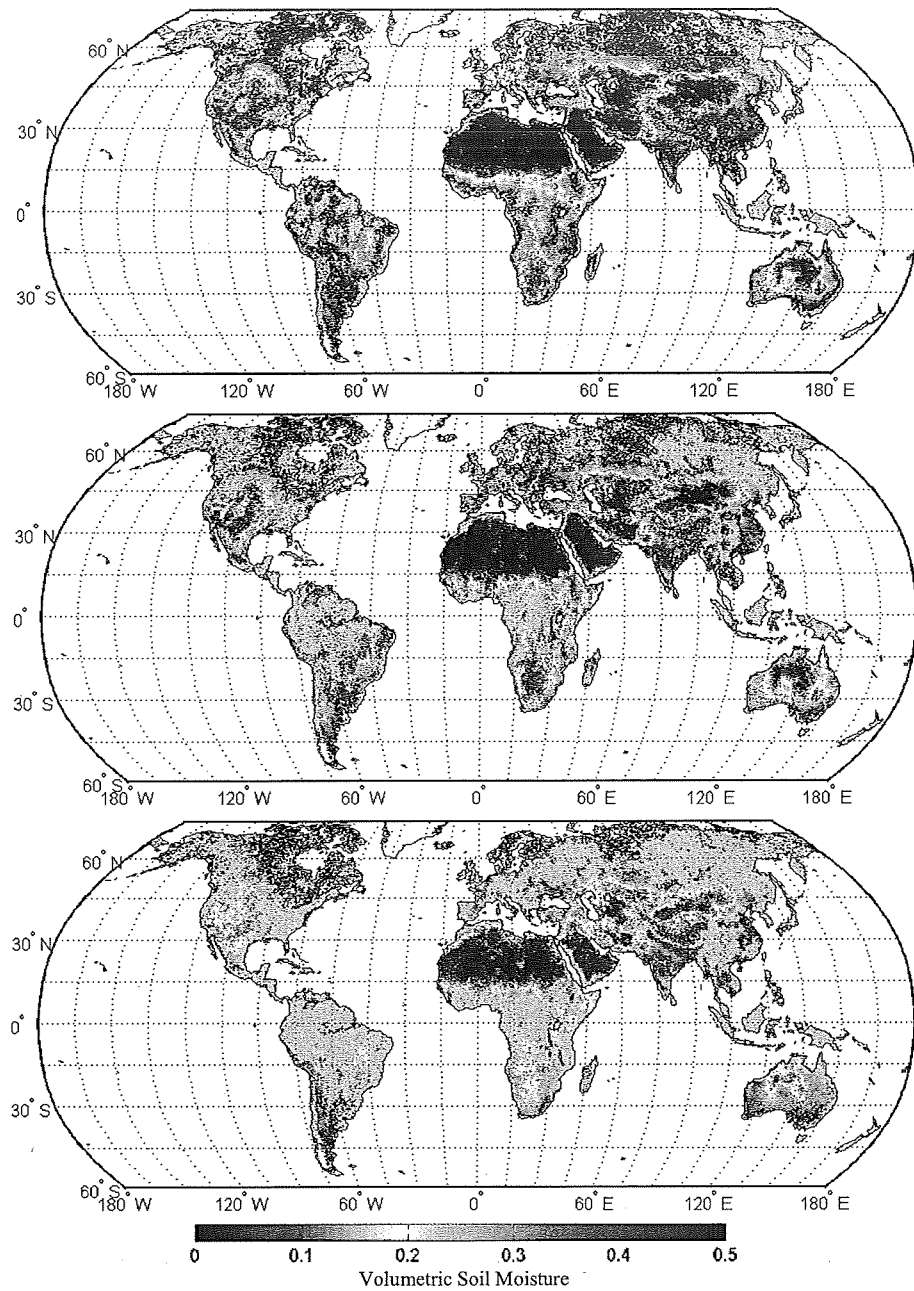
Instrument	Footprint Size (km) – (GHz)			
	6.x	10.7	18-19	36-37
SMMR	148 x 95	91 x 59	55 x 41	27 x 18
SSM/I	n/a	n/a	69 x 43	37 x 28
TMI	n/a	63 x 39	30 x 18	16 x 10
AMSR-E	74 x 43	51 x 30	27 x 16	14 x 8

Table 3. Equator crossing times for the DMSP satellite platforms

SSM/I Platform	Equator Crossing Times	
	Ascending Orbit	Descending Orbit
F-8	1812	0612
F-11	1710	0510
F-13	1735	0535
F-14	2021	0821
F-15	2131	0931
F-16	2013	0813



**Figure 1.** Twenty-four-hour day and night SMMR surface soil moisture retrievals for 7 July 1980.



**Figure 2.** Average monthly SMMR surface soil moisture retrievals at 6.6 GHz (top), 10.7 GHz (middle), and 18 GHz (bottom) for 7 July 1980.

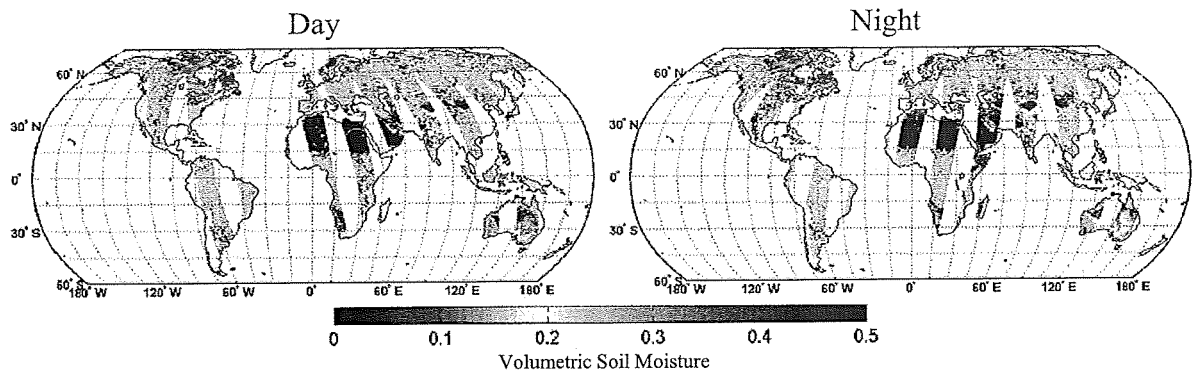


**Figure 3.** Twenty-four-hour day and night global SSM/I surface soil moisture retrievals for 7 July 2003.

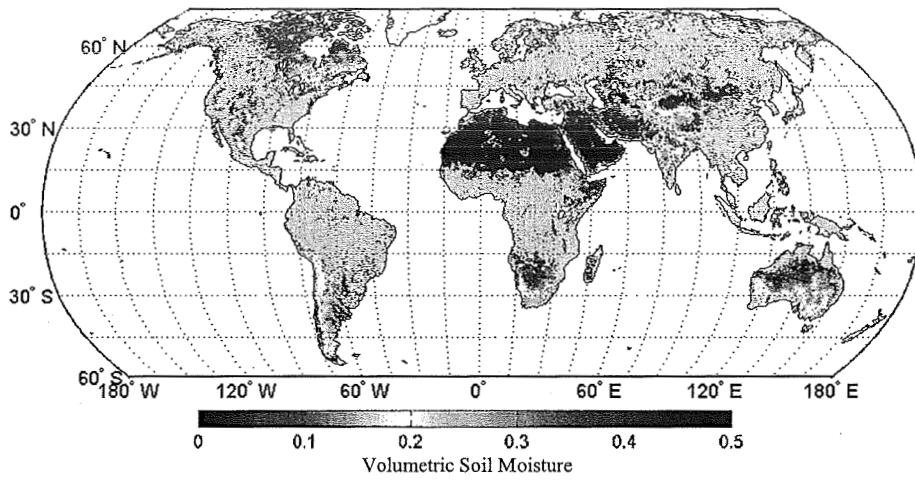


**Figure 4.** Monthly average global surface soil moisture for July 2003 as retrieved from SSM/I.

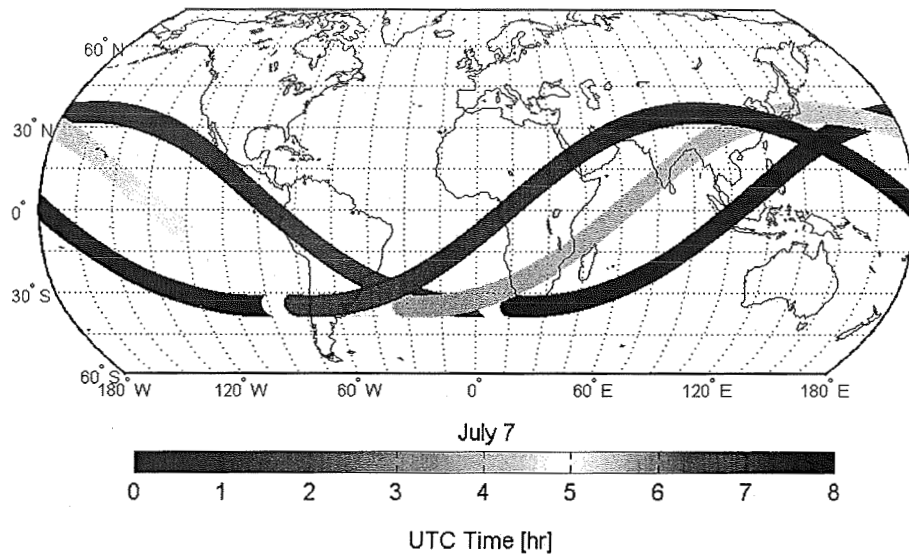


**Figure 5.** Selected TRMM orbit tracks during a 24-hour period, illustrating a typical pattern of daily coverage. A given daily pattern will repeat approximately every 47 days.

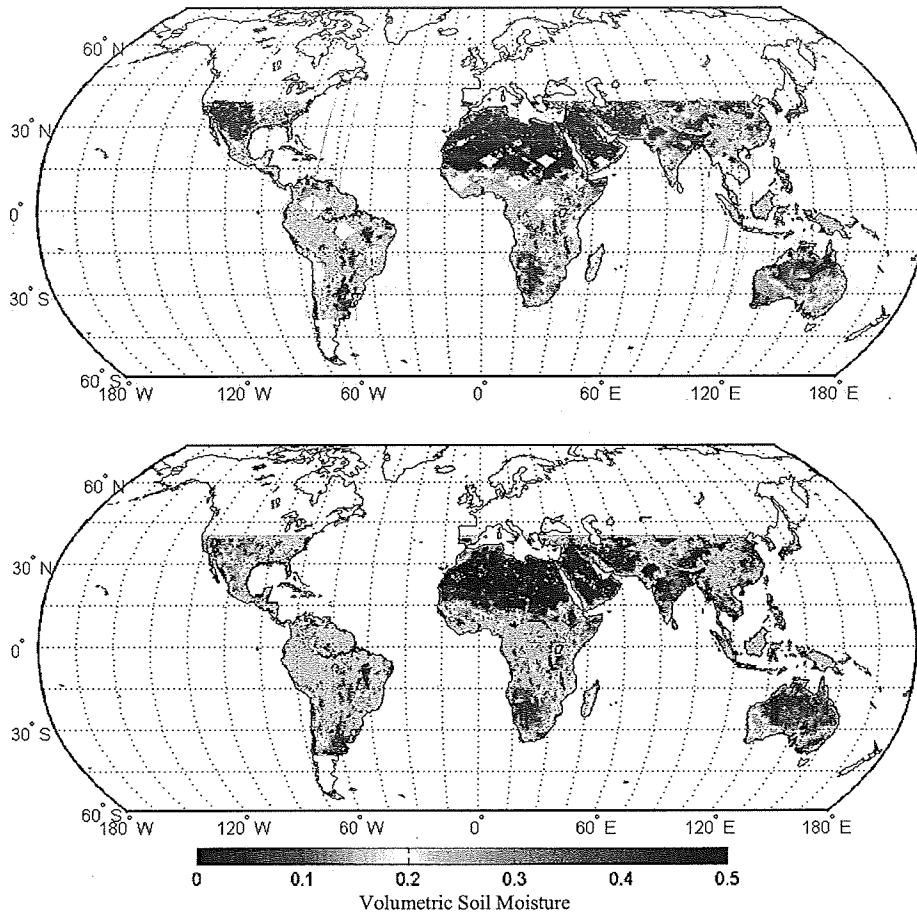


**Figure 6.** Twenty-four-hour and average monthly global surface soil moisture retrievals for 7 July (top) and July (bottom) 2003, derived from TMI at 10.7 GHz.



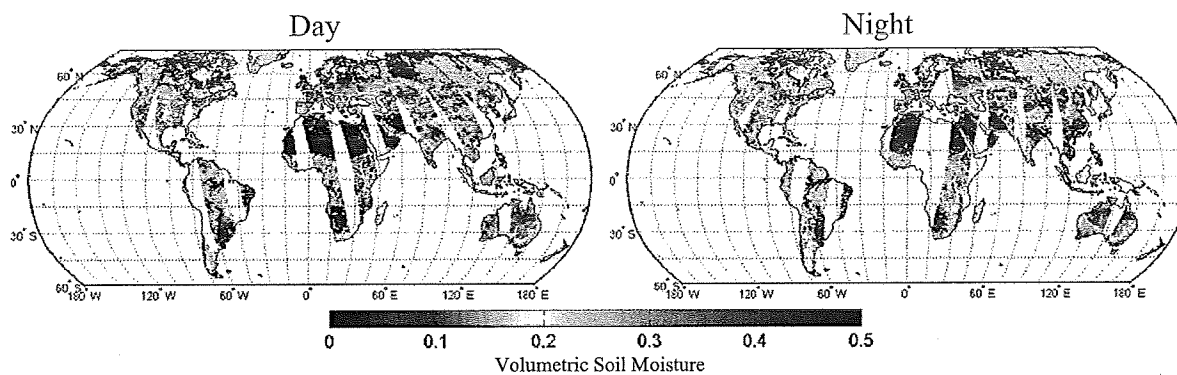


**Figure 7.** Twenty-four-hour global daytime and nighttime surface soil moisture retrievals at 6.9 GHz from AMSR-E.

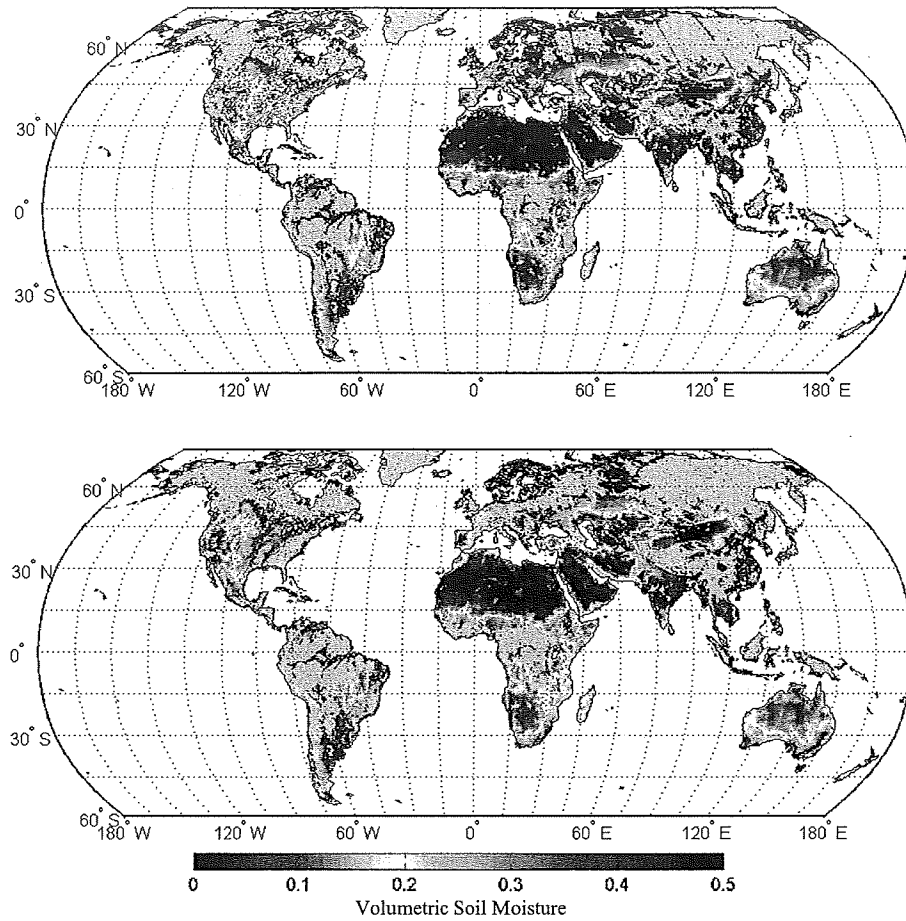


**Figure 8.** Average monthly global surface soil moisture retrievals at 6.9 GHz (top) and 10.7 GHz (bottom) from AMSR-E for July 2003.